Can Solventless Reactions Sometimes Succeed When Solvent-Mediated Reactions Fail? A Second Case Study for Cu(I) and Ag(I) Complexes of Divergently-Bridging Diimines without or with Fluorinated Azolates

Ruaa M. Almotawa,[†,‡] Christopher Hu,[†] Alessandro Cimino,[†] Vladimir N. Nesterov,[†] Mohammad A. Omary, [†,#] and Manal A. Rawashdeh-Omary [‡,*]

[†] *Department of Chemistry, University of North Texas, Denton, Texas 76203-5070*

[‡] *Departments of Chemistry and Biochemistry, Texas Woman's University, Denton, Texas, 76204*

[#] *Department of Chemistry, Yarmouk University, Irbid 21163, Jordan*

*: *Corresponding author. E-mail: momary@twu.edu (M. A. R.-O.)*

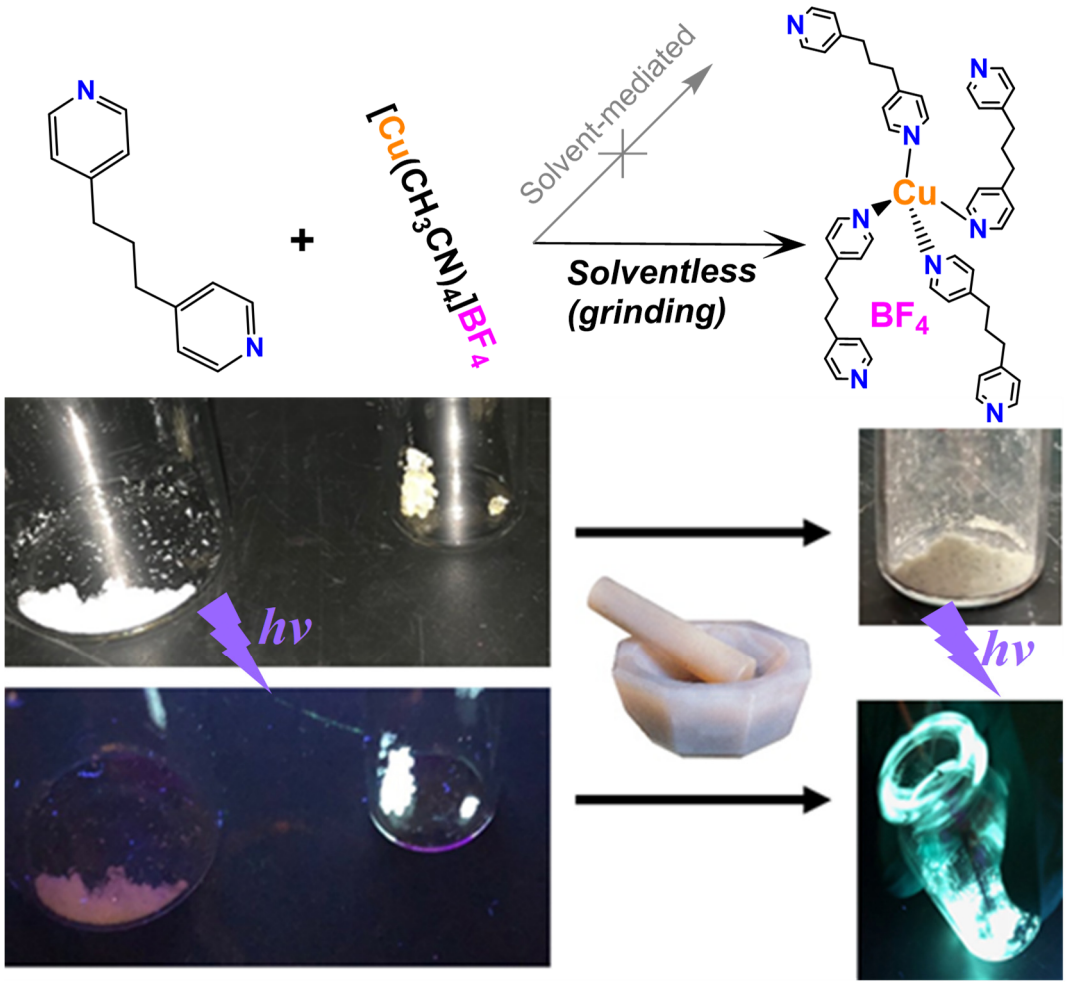

Abstract: This paper provides a 5th manifestation of a new tradition by which the editors of *Comments on Inorganic Chemistry* wish to lead by example, whereby we start publishing original research content that, nonetheless, preserves the Journal's identity as a niche for critical discussion of contemporary literature in inorganic chemistry. (For the previous manifestations, see: *Comments Inorg. Chem.* **2018**, *38*, 1-35; **2019**, *39,* 1-26; **2019**, *39,* 188-215; **2020**, *40*, 1-24.) Herein, synthetic details, solid-state structures, and photophysical properties of a group of silver(I) and copper(I) complexes are described. Two silver-based coordination polymers have been obtained: $\{[3,5\text{-}(CF_3)_2Pz]_2(bpp)Ag_2\}_\infty$ (**1**) and $\{[3,5\text{-}(CF_3)_2Pz][5\text{-}(C_6F_5)Ttz](bpp)Ag\}_\infty$ (**2**) -- constructed from bent 1,3-bis(4-pyridyl)propane (bpp), 3,5-bis(trifluoromethyl)pyrazole ($[3,5\text{-}(CF_3)_2Pz]H$) and 5-pentafluorophenyl-tetrazole ($[5\text{-}(C_6F_5)Ttz]H$) in order to inspect the influence of mixed ligands on the resulting silver-based coordination complexes. The structure of **1** shows a distorted trigonal planar geometry with both the bpp and $[3,5\text{-}(CF_3)_2Pz]$ ligands binding to the silver atom. The silver in **2** shows an uncommon interaction with the three different ligands. Also, two different geometries including distorted tetrahedral and distorted trigonal were presented for two different silver atoms. An interesting result was obtained for the Cu(I) coordination polymer $\{[Cu(bpp)_2][BF_4]\}_\infty$ (**3**) which was successfully synthesized in a solventless reaction but not a solvent-mediated reaction, hence manifesting a "green" chemistry route. The structure of **3** shows an ideal tetrahedral geometry similar to that for the silver analogue, $\{[Ag(bpp)_2][BF_4]\}_\infty$ (**3a**), published previously, whereas herein we obtained the same product with the same crystal structure via a more facile conventional synthetic route. All four complexes show bpp ligand-centered green emissions at ambient and cryogenic temperatures. Finally, a commentary is added to contrast the solventless vs solvent mediated reactions in both this investigation and a precedent thereof by the same corresponding author's group (*Inorg. Chem.* **2018**, *57*, 9962–9976), whereby reactions

proceeded successfully only *via* the solventless route through mechanical grinding herein and spontaneous sublimation by vapor diffusion from the solid-state of one reactant to another yet non-volatile reactant in the literature precedent, respectively.

Introduction

After the massive progress chemists have been making in the field of metal-organic frameworks (MOFs), the general area of coordination chemistry has been attracting ever increasing attention. The structure of coordination polymers (CPs) -- porous MOFs or otherwise non-porous congeners thereof -- is influenced by the geometries of metal centers and the divergently-bridging ligands.[1] A wide variety of organic linkers, including *N*-donor linkers such as azolate and diimine ligands, has been utilized with metal centers from across the periodic table. Rigid bidentate *N*-donor ligands, such as 4,4'-bipyridine, have been studied intensely as building blocks to connect the metal centers in order to form extended CPs, coordination oligomers, and other supramolecular architectures.[2] Flexible bidentate *N*-donor ligands, instead, attracted less attention, initially.[1g,3] Many highly-branched ligands usually show strong intermolecular interactions, resulting in the decline of the luminescence quantum efficiency due to their non-conjugated cores.[4] However, recently, conformationally-flexible ligands have been reported to exhibit distinctive crystalline architectures of their coordination polymers *en route* to attaining zeolite-like materials in the

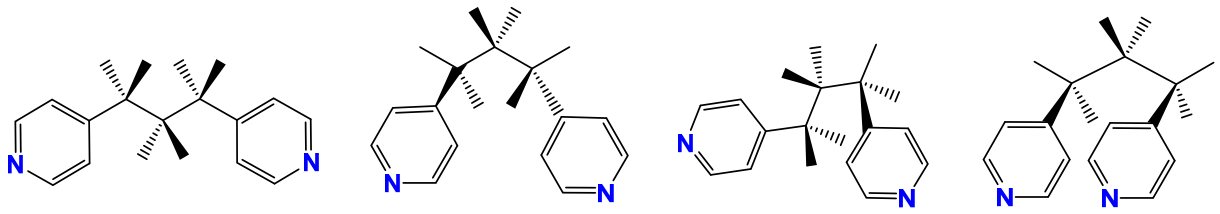

TT 9.1-10.1Å **GG` 6.7-8.6Å** **TG 8.6-9.2Å** **GG 3.9Å**

Chart 1

resulting MOFs toward ion exchange and catalysis, in addition to the novel topologies perceived from such species through the coordination with coinage metal centers in particular.[3g] The flexible ligand, 1,3-bis(4-pyridyl)propane (bpp), for example, can adopt different conformations (TT, TG, GG and GG') by changing N−N distances via rotating the pyridyl rings and the $(CH_2)_3$ groups (Chart 1).[3g] A number of products display an $M(bpp)_2$ stoichiometry with bpp ligands assuming only the three possible conformations (TT, TG, and GG').[3g] The unique case of $[Cu(II)(NO_3)_2(bpp)]_2.2CH_2Cl_2$ shows the GG conformation of the bpp ligand, which is very rare.[3g] Many papers represented the polymeric networks from silver(I) and bpp in term of the crystal engineering. Carlucci et al. have investigated different coordination frames of $[Ag(bpp)_2]X$ upon the variation of the counter ions, where X = NO_3, BF_4, ClO_4, PF_6, or AsF_6.[3g] Kokunov et al. as well reported the double-helix framework of $[Ag(bpp)_2]X$, where X = CF_3COO.[5] Those papers suggested that different anions would impact the bpp conformation because the arrangement of the ligands' coordination modes and the anions' supramolecular interactions assists to build up the crystal structures of such complexes in different ways. The intended "counterions" in the design have proven to be present in three different modes: coordinated, uncoordinated, or mixed modes.[6] The dimensionality of the structures commonly increases with the coordinated anions, whereas the uncoordinated anions facilitate to extend the structures by other weak bonding or attractive forces, including hydrogen bonding, π-π stacking, metal···metal (metallophilic), and/or metal-π (ligand) interactions.[6] Meanwhile, Shieh et al. have reported a family of liquid-assisted mechanically-ground semiconducting solids based on ternary Te-Fe-Cu carbonyl clusters and conjugation-interrupted dipyridyl linkers, two of which included Cu(I)-bpp moieties, including the $[Cu(bpp)_2]^+$ complex itself as a precursor, albeit its synthesis was not by mechanical grinding.[7] Coinage metal complexes with such ligands exhibit motivating features in the areas of supramolecular assembly,

acid−base chemistry, and metalloaromaticity.[7] The behavior of π-acid−base and cation−π interactions for coinage metal metallocyclic complexes depends mainly on the metal and the nature of the organic linkers, which in our case are diimine, pyrazolate and/or tetrazolate ligands. The monovalent coinage metal complexes of pyrazolate and triazolate ligands have been studied intensively in recent years.[8] Dias et al. reported the synthesis and characterization of silver(I) and copper(I) adduct of the 3,5-bis(trifluoromethyl)pyrazolate ligand, $[3,5(CF_3)_2Pz]^-$.[9] The remarkable properties of the trinuclear silver(I) pyrazolate $[Ag^I(3,5\text{-}(CF_3)_2pz)]_3$ were described in our laboratory through luminescence on/off switching causing by vapochromic selective sensing of hazardous and highly regulated small-organic-molecule vapors such as benzene.[10] The intercalation of guest molecules between the ladders of trimer units can identify this phenomena.[9] Relatively, tetrazole chemistry has urged the researchers in the last two decades by a plethora of applications in different fields, including biomedical and coordination chemistry.[11] One of the most remarkable fluorinated tetrazolate ligands that is commercially available is 3,5-$(CF_3)_2$-Ph-5-tetrazole (BTFTH) (Chart 2).[12] It has been used as an activator in RNA synthesis and as luminophore in organic light-emitting diodes (OLEDs).[11] Notably, introducing electron-withdrawing groups such as CF_3 or fluorine atoms to aryl groups can increase the thermal and oxidative stability and reduce the quenching of metal complexes or coordination polymers.[13] Gerhards et al. described the syntheses and coordination chemistry of some of the fluorinated tetrazolate with Ag(I) and Cu(II).[11d] However, not all the fluorinated tetrezolate ligands are well-studied regarding their reactivity and coordination to the metals. Due to the great consideration in the design of coordination polymers and their significance, several methods can manifest the synthesis -- one of which is a solventless reaction that has been discussed in detail in

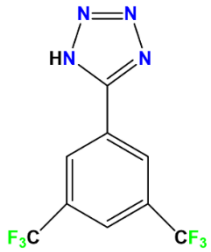

BTFTH

Chart 2

our previous work as well as work by other groups.[14] Our main purpose in adopting the solventless route is to expand the area of "green synthesis" to reduce the use of toxic and volatile organic solvents -- particularly benzene and dichloromethane, which pose a serious threat to the health and environment. Solventless or solid state reactions are carried out by grinding or subliming the reactants together, depending on the properties of the ligand or metal precursors. Metal complexes including two or more different ligands bonded to the metal ion are designated as mixed-ligand complexes. This type of complexes has also been called "ternary complexes" for example when the ligands are studied in biochemical systems as components of multimetal-multiligand species.[15] Coordination complexes with mixed ligands afford a variety of fascinating applications related to the construction of three-dimensional metal-organic frameworks (3D-MOFs) with different structural topologies, coordination geometries/modes, and structural conformations of ligands. Such structural topologies have been built by binding one metal center to two different ligands such as diaza-base and multi-carboxylate ligands.[16]

With all the aforementioned attributes in mind, we have sought to investigate a series of homoleptic and heteroleptic Ag(I) and Cu(I) coordination polymers. To further discover the coordination opportunities of the flexible and rigid bidentate ligands with monovalent silver or copper metals, bpp was used as a primary ligand followed by a fluorinated pyrazolate and/or a fluorinated tetrazolate secondary ligand(s) to construct the CPs and investigate their photophysical properties. One added objective for this paper is to study the effect of reducing the symmetry of metal complexes by increasing the number of ligands surrounding the metal center. Also, we will illustrate the environmentally-friendly solventless methodology to synthesize stable metal complexes.

Results and Discussion

Synthesis and Reactivity. The neutral coordination polymer $\{[3,5\text{-}(CF_3)_2Pz]_2(bpp)Ag_2\}_\infty$ (**1**), is obtained in 80% yield by a reaction between the trinuclear silver(I) complex $\{[3,5\text{-}(CF_3)_2Pz]Ag\}_3$ and the diimine ligand (bpp) in dichloromethane. The other neutral coordination polymer, $\{[3,5\text{-}(CF_3)_2Pz][5\text{-}(C_6F_5)Ttz](bpp)Ag\}_\infty$ (**2**), can be prepared by adding the fluorinated tetrazole [5-(C_6F_5)Ttz]H to the previous reaction of $\{[3,5\text{-}(CF_3)_2Pz]Ag\}_3$ and bpp in methanol in the presence of the Et_3N base to deprotonate the tetrazole and attain a tetrazolate ligand. The third complex is the Cu(I) coordination polymer $\{[Cu(bpp)_2][BF_4]\}_\infty$ (**3**). We were not successful to obtain complex **3** by the conventional solvent-mediated method due to the high air sensitivity of Cu(I) in solution. However, surprisingly, by using the same solventless approach discussed in our previous paper,[13] we have been able to obtain a very stable compound with bright solid-state photoluminescence among other desirable photophysical properties only upon grinding the copper precursor -- tetrakis(acetonitrile)copper(I) tetrafluoroborate, $[Cu^I(MeCN)_4][BF_4]$ -- with the bpp ligand. However, we have not been able to reproduce the silver complexes by solventless methods. We have been able to reproduce the synthesis and structure of the silver analogue of complex **3**, i.e. $\{[Ag(bpp)_2][BF_4]\}_\infty$ (**3a**), via a different procedure from that used in the literature.[3g] Whereas in ref. 3g methanol and CH_2Cl_2 were used in the synthesis and crystals were obtained upon layering the two reactants $AgBF_4$ and bpp in the aforementioned solvents, respectively, herein we followed a normal synthetic route by mixing the reactants in toluene then we obtained crystals from an acetonitrile solution of the crude product. In the remainder of this paper, we emphasize only the non-redundant findings about complexes **3** and **3a** such as their synthetic procedure differences from the literature and luminescence properties, whereas we present comparisons with ref. 7 and

ref. 3g, respectively, for the structural details since our crystal structures were essentially identical despite the starkly different and simpler synthetic routes herein.

Several attempts to obtain Cu(I) analogues of complex **1** and **2** were made; however, no new products were produced, underscoring the greater propensity of Ag(I) to attain heteroleptic complexes. All three complexes are insoluble in most common organic solvents at room temperature. Complexes **1** and **3** are soluble in acetonitrile after heating and sonication, whereas complex **2** is partially soluble in dimethyl sulfoxide (DMSO), dimethylformamide (DMF) and acetonitrile (ACN) after heating and sonication. The ultimate crystallization products were obtained from acetonitrile by the slow evaporation method. All silver complexes are air-stable solids as well as solutions at ambient conditions, but they are light-sensitive in solution. The copper complex is an air-stable solid but unstable in solution. All three complexes are green-luminescent.

Single crystals of all three samples were obtained and their structures determined by X-ray crystallographic analysis. In **3**, the Cu(I) atoms are connected to the diimine ligand (bpp), which acts as the bridging ligand to form the coordination polymer. However, in **1** and **2**, the Ag(I) atoms are connected to the pyrazolate and tetrazolate, which act as chelating ligands. The type and the number of ligands surrounding the Ag(I) atoms can affect the conformations of bpp ligands, as will be explained in the subsequent X-ray section.

X-ray Crystal Structures. Colorless single crystals of each complex were obtained from acetonitrile. Molecular and packing structures are shown in Figures 1-3. Tables 1 and 2 list selected X-ray crystallographic data for all three complexes.

The molecular structure of complex **1**, $\{[3,5\text{-}(CF_3)_2Pz]_2(bpp)Ag_2\}_\infty$, was solved in the tetragonal space group $P\bar{4}2_1c$ with Z = 4 in the unit cell. Silver(I) coordinates to two nitrogen atoms from different pyrazolate ligands and one nitrogen atom from one pyridyl group in the bpp ligand to form a dinuclear repeat unit with two three-coordinate Ag(I) centers. The packing structure shows extended chains with small porosity. The connection of Ag(I) atoms with the pyrazolate affects the bpp conformation – GG' – noticeably, here resulting in an N-to-N distance of 8.28 Å; see Table 3, Figure 1, and Charts 1 and 3. The N-to-N distance usually can be affected by even small deviations caused by rotating the angles,[3g] herein, when the silver atoms bind to small chelating ligands such as the pyrazolate in this compound. From a different viewpoint, the trimeric Ag(I) precursor complex with pyrazolate ligand breaks down into a dinuclear unit upon binding to a "back-to-back" di(4-pyridyl) linearly-bridging ligand (bpp). These dimeric units are connected together by the bpp ligand to form a coordination polymer. Such ligands could breakdown the trimeric units to form dinuclear complexs, e.g. $\{[3,5\text{-}(CF_3)_2Pz]M(2,4,6\text{-collidine})\}_2$, M=Cu(I) and Ag(I), that was reported upon the reaction of the trimeric Ag(I) and Cu(I) complexes with 2,4,6-collidine.[7g] However, no coordination polymers have been reported because the collidine ligand has one nitrogen atom acting as a site of coordination, unlike the back-to-back diimine ligands herein that have two coordination sites as divergently-bridging bidenate.

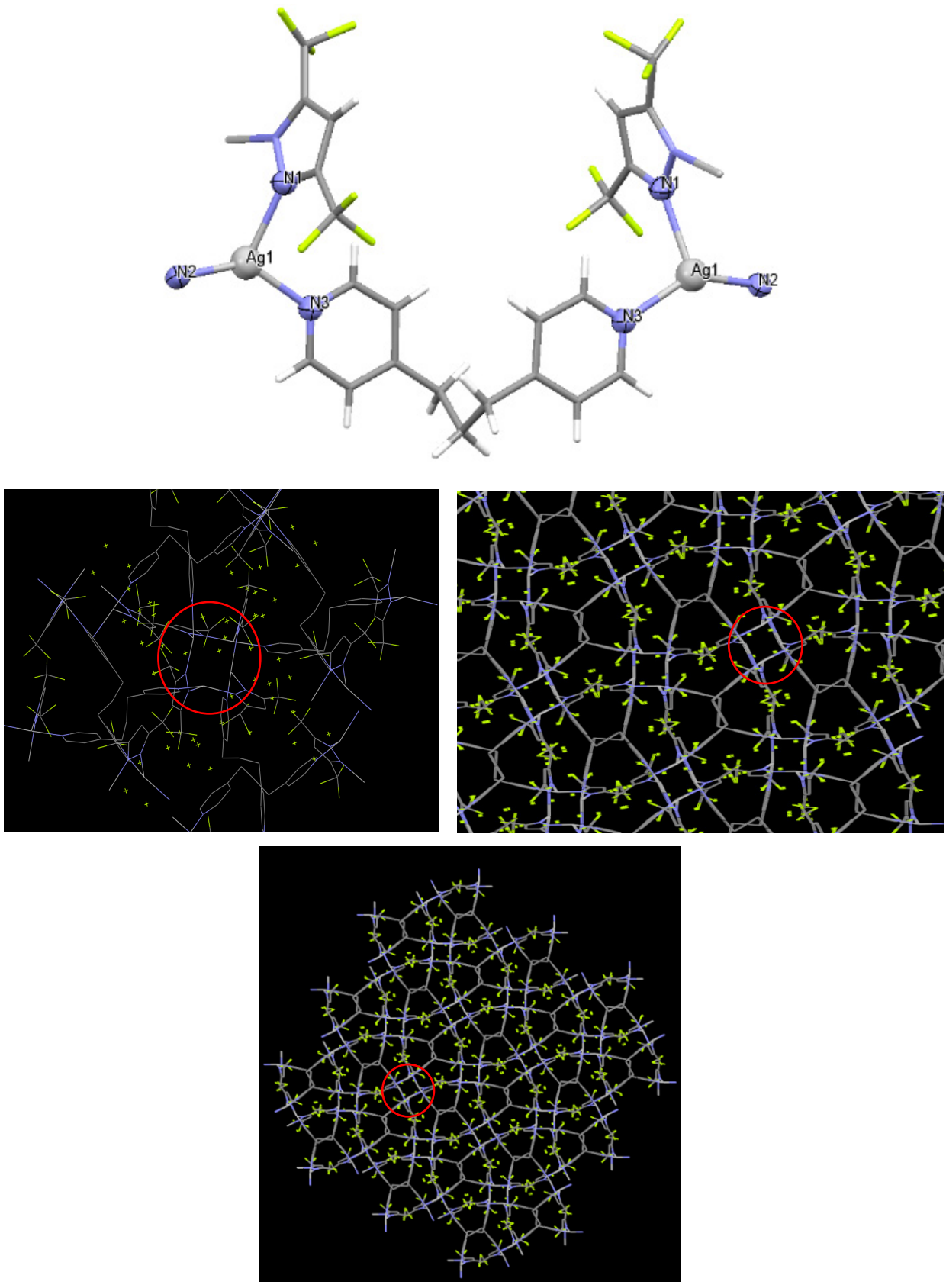

Figure 1. The molecular and packing structures for {[3,5-$(CF_3)_2$Pz]Ag}$_2$bpp.

The molecular structure of complex **2**, $\{[3,5\text{-}(CF_3)_2Pz][5\text{-}(C_6F_5)Ttz](bpp)Ag\}_\infty$, was solved in the triclinic space group $P\bar{1}$ with Z = 2 in the unit cell. In the molecular structure, two silver(I) atoms exist. The Ag1 atom coordinates to three nitrogen atoms from the three different ligands -- i.e., one nitrogen atom each from the pyrazolate, tetrazolate, and one pyridyl group within the bpp ligands, to form a three-coordinate Ag(I) center. The three distances of Ag1-N are not exactly the same and likewise for the angles around silver atoms in the coordination sphere (2.18, 2.21, 2.35 Å and 100.73, 113.08, 146.02°, respectively; see Table 2) -- consistent with the AgN_3 core exhibiting a distorted trigonal-planer structure (Figure 2). The Ag2 atom, in contrast, coordinates to four nitrogen atoms, comprising two from two different tetrazolate ligands, one from the pyrazolate ligand, and one from the bpp ligand, to form a tetrahedral geometry with a high degree of distortion of N-Ag2 bond (2.58 Å). The four Ag2-N distances are different from one another (2.21, 2.22, 2.42, and 2.58 Å; i.e., 2.35 ± 0.18 Å). Likewise for the angles around silver atoms in the coordination sphere and (86.64, 102.13, 102.72, 108.29, 99.77 and 143.27°; i.e., 107.14 ± 19.11°) – see Table 2. These bond distance and bond angle values are consistent with the AgN_4 core exhibiting a distorted tetrahedral structure (Figure 2). The packing structure reveals two layers of extended chains. By increasing the number of ligands around the Ag(I) atoms, the N-to-N distance increases to 10.22 Å, leading to the longest bpp conformation (TT; see Table 3 and Figure 4). Although the bpp ligand has the longest N-N distance, the structure still shows a small surface area of 0.85 cm^3/g due to the large number of coordination sites from the tetrazolate ligands. Previous work was unable to characterize $[(BTFT)Ag^I]$ due to lack of solubility.[11d] It was concluded that this kind of materials tends to be amorphous.[11d] However, by introducing other ligands such as pyridine, a crystal structure from the analogous $[(BTFT)Cu^{II}]$ was obtained by recrystallization from pyridine to give purple crystals of the complex $[(BTFT)_2Cu(Py)_2]_n$.[11d]

Therefore, we obtained a crystal structure from {[3,5-$(CF_3)_2$Pz][5-(C_6F_5)Ttz](bpp)Ag}, due to the presence of the diimine ligand (bpp), despite the lack of solubility. Overall, complex **3** shows low symmetry via the different geometries of the silver(I) atoms upon binding to three different ligands.

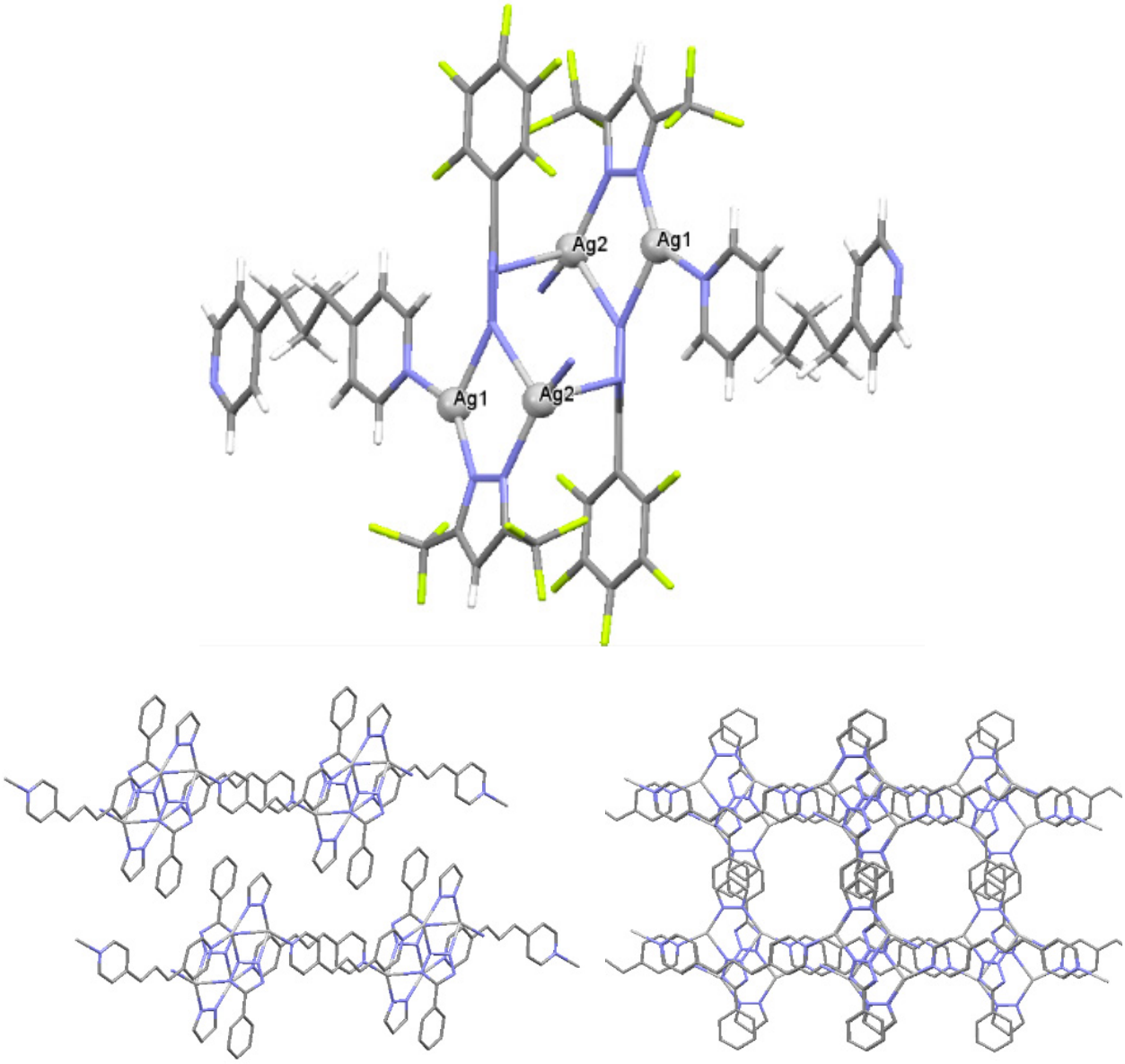

Figure 2. The molecular and packing structures for {[3,5-$(CF_3)_2$Pz][5-(C_6F_5)Ttz]Ag}bpp.

The colorless single crystals of complex **3**, $\{[Cu(bpp)_2][BF_4]\}_\infty$, were obtained from acetonitrile. Molecular and packing structures are shown in Figure 3. Table 1 lists selected X-ray crystallographic data for the complex. The molecular structure of $[Cu(bpp)_2](BF_4)$ was solved as tetragonal $I4_1/acd$ with Z = 8 in the unit cell. It features a nearly ideal tetrahedral structure. All the N–Cu–N angles are close to 109°. The Cu–N bond distances are 2.0522(10) Å. The N-to-N distance of the bpp ligand is 6.72 Å, leading to a GG' conformation. The deviation of the bpp conformation from linear mode (TT) to the bent mode (GG') could be due to the arrangement of the ligands' coordination modes and the anions' supramolecular interactions. These X-ray data are similar to those observed for the known silver analogue. [3g]

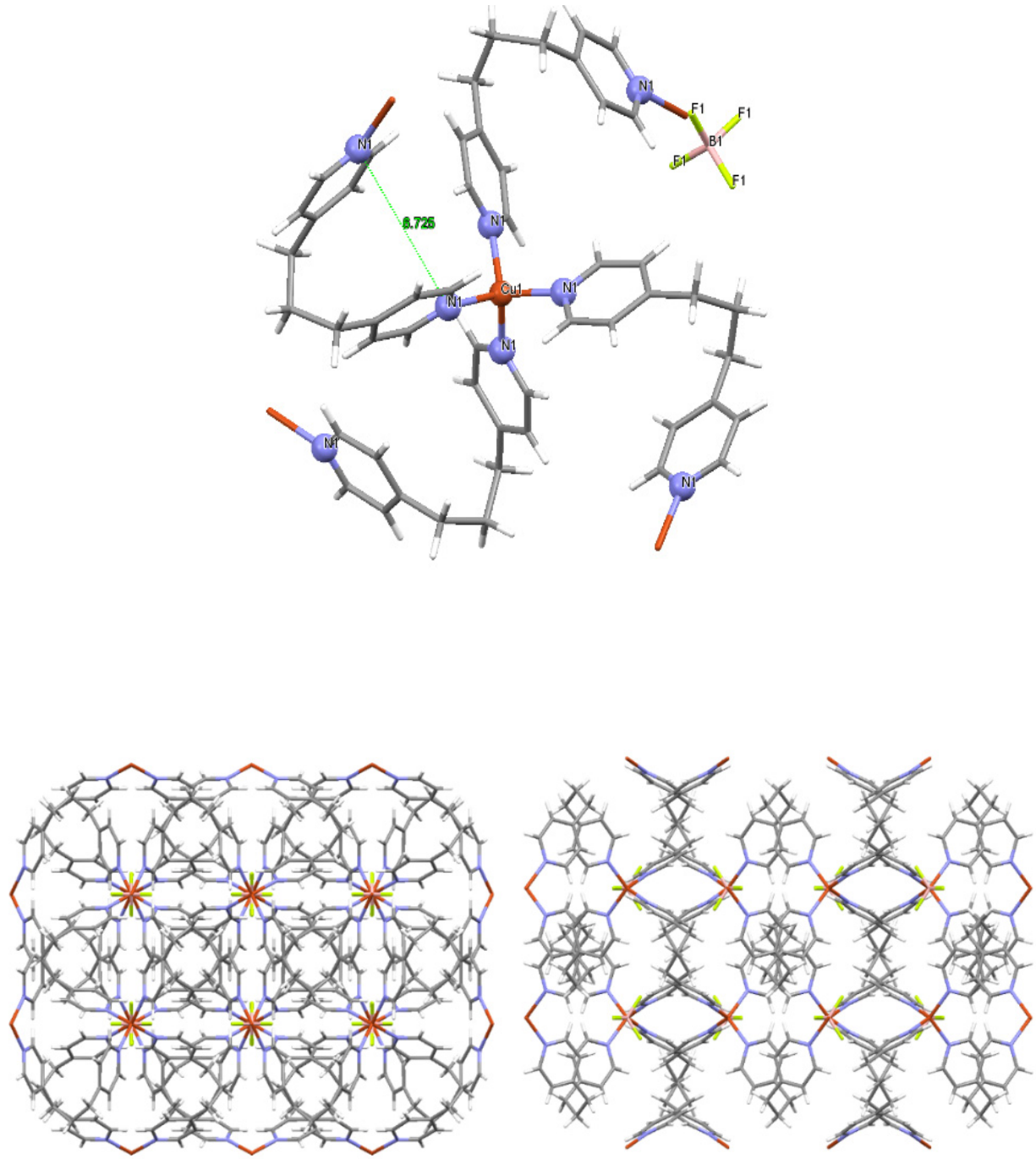

Figure 3. The molecular and packing structures for $[Cu(bpp)_2][BF_4]$.

Table 1. X-ray Crystallographic Data for All Complexes in This Study

	Complex 1/This work	***Complex 2/This work***	***Complex 3/This work***
CCDC	1873400	1873406	1873407
Crystal system	Tetragonal	Triclinic	Tetragonal
Formula	C_{23} H_{16} Ag_2 F_{12} N_6	C_{25} H_{15} Ag_2 F_{11} N_8	C_{26} H_{28} B Cu F_4 N_4
Formula weight	820.16	852.19	546.87
Space group	$P\bar{4}2_1c$	$P\bar{1}$	$I4_1/acd$
a, (Å)	14.5864(9)	10.5655(5)	14.3550(2)
b, (Å)	14.5864(9)	11.4770(6)	14.3550(2)
c, (Å)	12.8924(8)	12.5912(6)	24.0126(7)
α, (deg)	90°	108.418(1)	90°
β, (deg)	90°	102.081(2)	90°
γ, (deg)	90°	99.894(1)	90°
V, (Å^3)	2743.0(4)	1369.1(1)	4948.2(2)
Z	4	2	8
T, (K)	200(2)	220(2)	100.0 (1)
λ, (Å)	0.71073	0.71073	0.71073
ρ_{calcd}, (mg/m^3)	1.986	2.067	1.468
μ, (mm^{-1})	1.536	1.540	0.936
Crystal size, (mm^3)	0.287 x 0.22 x 0.11	0.149 x 0.142 x 0.117	0.1 x 0.07 x 0.055
Absorption correction	multi-scan	multi-scan	multi-scan
abs corr factor	0.7455/0.6504	0.7465/0.6750	1.0000/ 0.9084
Total reflections	32531	37601	11558
Independ. Reflections	3030	6045	1479
Data/res/parameters	3030 / 178 / 238	6045 / 0 / 416	1479 / 0 / 83
R1 [I > 2σ(I)]	0.0237	0.0236	0.0247
wR2 [I > 2σ(I)]	0.0661	0.0569	0.0706
R1 (all data)	0.0254	0.0267	0.0267
wR2 (all data)	0.0680	0.0584	0.0720
GOF on F^2	1.060	1.111	1.047
Δρ(max), Δρ(min) (e/Å^3)	0.458, -0.363	0.475, -0.344	0.372, -0.377

	Complex 3a/This work	***Complex 3/Ref. 7***	***Complex 3a/Ref. 3g***
CCDC	1873399	1537068	178925
Crystal system	Tetragonal	Tetragonal	Tetragonal
Formula	C_{26} H_{28} Ag B F_4 N_4	C_{26} H_{28} B Cu F_4 N_4	C_{26} H_{28} Ag B F_4 N_4
Formula weight	591.20	546.87	591.20
Space group	$I4_1/acd$	$I4_1/acd$	$I4_1/acd$
a, (Å)	14.6438(14)	14.4223(4)	14.703(4)
b, (Å)	14.6438(14)	14.4223(4)	14.703(4)
c, (Å)	24.272(5)	24.1321(8)	24.304(4)
α, (deg)	90°	90	90
β, (deg)	90°	90	90°
γ, (deg)	90°	90	90
V, (Å^3)	5205.0(2)	5019.5(3)	5254(2)
Z	8	8	8
T, (K)	220(2)	200(2)	293(2)
λ, (Å)	0.71073	0.71073	0.71073
ρ_{calcd}, (mg/m^3)	1.509	1.447	1.495
μ, (mm^{-1})	0.825	0.922	0.817
Crystal size, (mm^3)	0.159 x 0.114 x 0.085	0.25 x 0.18 x 0.04	0.26 x 0.24 x 0.20
Absorption correction	multi-scan	Semi-empirical from equivalents	Psi-scan
abs corr factor	0.7455/0.6588	0.9640/0.8022	1.00/0.96
Total reflections	32771	7503	2507
Independ. Reflections	1450	1116	1293
Data/res/parameters	1450 / 0 / 87	1116/0/83	1293/0/83
R1 [I > 2σ(I)]	0.0242	0.0313	0.0359
wR2 [I > 2σ(I)]	0.0626	0.0847	0.0623
R1 (all data)	0.0312	0.0470	0.1859
wR2 (all data)	0.0695	0.0957	0.0842
GOF on F^2	1.047	1.015	0.896
Δρ(max), Δρ(min) (e/Å^3)	0.322, -0.445	0.385, -0.293	0.253, -0.269

$R_1 = \Sigma||F_o| - |F_c||/\Sigma|F_o|$; $wR_2 = \{\Sigma[w(F_o^2 - wF_c^2)^2/\Sigma[w(F_o^2)^2]\}^{1/2}$

Table 2. Selected Bond Lengths (Å), Intramolecular Contacts (Å) and Angles (°) for **1** - **3** & **3a**

1/This work		**2/This work**		**3/This work**	
Ag(1)-Ag(1)#1	3.2662(6)	Ag(1)-N(1)	2.3509(19)	Cu(1)-N(1)#1	2.0522(10)
Ag(1)-N(1)	2.324(3)	Ag(1)-N(5)	2.2166(18)	Cu(1)-N(1)	2.0522(10)
Ag(1)-N(2)#2	2.187(4)	Ag(1)-N(6)	2.1792(18)	Cu(1)-N(1)#2	2.0522(10)
Ag(1)-N(3)	2.241(4)	N(5)-Ag(1)-N(1)	100.70(7)	Cu(1)-N(1)#3	2.0522(10)
N(3)-Ag(1)-Ag(1)#1	119.72(10)	N(6)-Ag(1)-N(1)	113.10(7)	N(1)#1-Cu(1)-N(1)#2	109.05(3)
N(1)-Ag(1)-Ag(1)#1	114.42(9)	N(6)-Ag(1)-N(5)	146.03(7)	N(1)#1-Cu(1)-N(1)	109.05(3)
N(2)#2-Ag(1)-Ag(1)#1	64.36(10)	N(2)-C(1)-C(2)	123.3(2)	N(1)#1-Cu(1)-N(1)#3	110.31(5)
N(2)#2-Ag(1)-N(1)	110.88(13)	N(2)-C(1)-N(3)	112.4(2)	N(1)#1-Cu(1)-N(1)#2	109.05(3)

Symmetry transformations used to generate equivalent atoms:

Complex **1**: #1 -x+2,-y+2,z #2 -y+2,x,-z

Complex **3**: #1 -y+1/4,x+1/4,-z+3/4 #2 -x+0,-y+1/2,z+0 #3 y-1/4,-x+1/4,-z+3/4.

3a/This work		**3/Ref. 7**		**3a/Ref. 3g**	
Ag(1)-N(1)#1	2.3146(14)	Cu(1)-N(1)	2.053(2)	Ag(1)-N(1)	2.317(4)
Ag(1)-N(1)#2	2.3146(14)	Cu(1)-N(1)#3a	2.053(2)	Ag(1)-N(1)#1b	2.317(4)
Ag(1)-N(1)#3	2.3146(14)	Cu(1)-N(1)#5a	2.053(2)	Ag(1)-N(1)#2b	2.317(4)
Ag(1)-N(1)	2.3146(14)	Cu(1)-N(1)#6a	2.053(2)	Ag(1)-N(1)#3b	2.317(4)
N(1)#1-Ag(1)-N(1)#2	108.94(3)	N(1)-Cu(1)-N(1)#5a	109.15(5)	N(1)-Ag(1)-N(1)#1b	108.8(1)
N(1)#1-Ag(1)-N(1)	108.94(3)	N(1)#3a-Cu(1)-N(1)#5a	109.15(5)	N(1)-Ag(1)-N(1)#2b	108.8(1)
N(1)#1-Ag(1)-N(1)#3	110.53(7)	N(1)-Cu(1)-N(1)#6a	109.15(5)	N(1)#1b-Ag(1)-N(1)#2b	110.9(2)
N(1)#3-Ag(1)-N(1)	108.94(3)	N(1)#3a-Cu(1)-N(1)#6a	109.15(5)	N(1)-Ag(1)-N(1)#3b	110.9(2)
N(1)#2-Ag(1)-N(1)	110.53(7)	N(1)-Cu-N(1)#3a	110.1(1)		
N(1)#2-Ag(1)-N(1)#3	108.94(3)	N(1)#5a-Cu-N(1)#6a	110.1(1)		

Symmetry transformations used to generate equivalent atoms:

Complex **3a**/This work: #1 -y+3/4, x-1/4, -z+1/4 #2 -x+1, -y+1/2, z+0 #3 y+1/4, -x+3/4, -z+1/4

Ref. 7: #3a -x+1, -y+1/2, z+0 #5a y+1/4, -x+3/4, -z+1/4 #6a -y+3/4, x-1/4, -z+1/4

Ref. 3g: #1b y+3/4, -x+5/4, -z+3/4 #2b -y+5/4, x-3/4, -z+3/4 #3b -x+2, -y+1/2, z

Table 3. Conformation parameters for bpp in the coordination polymers herein.

Complex	Formula	Conformation	N-to-N/ Å
1	{[3,5-$(CF_3)_2$Pz]Ag}$_2$bpp	GG'	8.28
2	{[3,5-$(CF_3)_2$Pz][5-(C_6F_5)Ttz]Ag}bpp	TT	10.22
3	[Cu$(bpp)_2$]BF_4	GG'	6.72
3a	[Ag$(bpp)_2$]BF_4	GG'	6.66
3/ref. 7	[Cu$(bpp)_2$]BF_4	GG'	6.75
3a/ref. 3g	[Ag$(bpp)_2$]BF_4	GG'	6.68

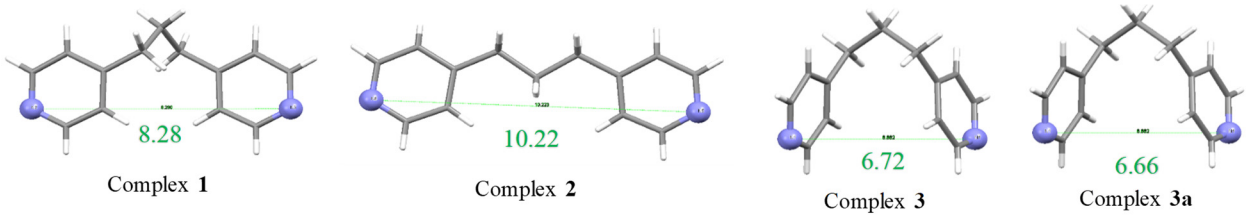

Complex **1** Complex **2** Complex **3** Complex **3a**

Chart 3. Illustration of the bpp conformations in the coordination polymers herein, whose parameters are shown in Table 3.

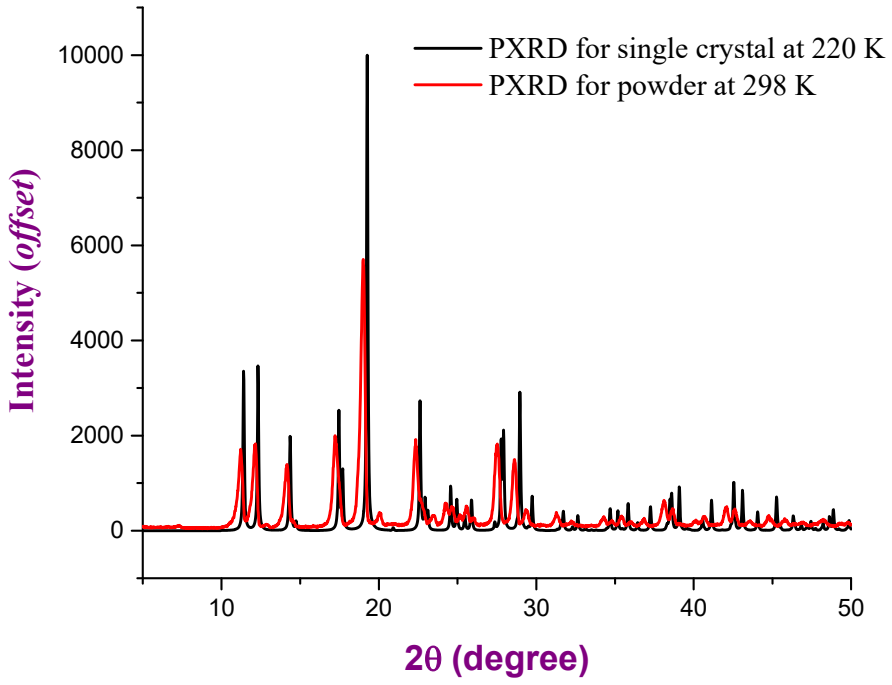

Figure 5. PXRD patterns for **3** in various solid forms; powder and single crystal.

The solventless transformation attains a crystalline product of **3** with powder X-ray diffraction (PXRD) patterns similar to the simulated PXRD pattern for the single crystals. Thus, Figure 5 shows that both the powder and the single crystal are highly crystalline. Starting with the $[Cu(MeCN)_4][BF_4]$ precursor, adding two equivalents of bpp in a closed vessel attains a light green product upon mechanical grinding of bpp from its solid form into the copper precursor at ambient conditions. The evidence of the reaction was the appearance of a bright green luminescence immediately while grinding. In contrast, when the reaction was attempted under solvent-mediated conditions, an unstable Cu(I) product was obtained that immediately underwent oxidation.[13] Crystals were easily formed from acetonitrile for the solventless product to attain the 4-coordinate cationic coordination polymer. Several attempts were unsuccessful to obtain a product by grinding analogous silver(I) precursor salts or trimer with the bpp ligand.

Spectroscopic Characterization.

Table 4. Summary of photophysical parameters for all complexes in this study.

	$\lambda_{exc\ (max)}$ (nm)		$\lambda_{em\ (max)}$ (nm)		τ (μs)	
Temp.	298 K	77 K	298 K	77 K	298 K	77 K
*Complex **1***	280	275	500	520	35.34	111
*Complex **2***	280	280	500	525	35.31	111.3
*Complex **3***	365	365	500	515	11.24	19.26
$[Ag(bpp)_2][BF_4]$	330	335	500	510	12.58	16.82

τ = photoluminescence lifetime at the characteristic λ_{max}.

It is well-known that d^{10} metal ions of group 11 with selected ligands exhibit novel luminescence materials with fascinating properties.[1g,17] Herein, all the silver(I) coordination polymers show bright green luminescence upon exposure to UV radiation. Table 4 summarizes the photophysical data while Figures 6 and 7 illustrate the solid-state luminescence spectra for single crystals of the three compounds in this paper beside the silver analogue, $[Ag(bpp)_2][BF_4]$, **3a**, at room temperature and 77 K. The luminescence energies in the green region and unstructured spectral profile are rather similar for all complexes (Table 4 and Figures 6-9). The experimental lifetimes are in the microsecond scale, suggesting phosphorescence. The dipyridyl ligand (bpp) alone exhibits an excitation peak at 427 nm and a maximum emission peak at 522 nm at 77 K attributed to π-π* transitions (Figure 8). For complexes **1** and **2**, by comparing their luminescence data, they show similar results with an excitation at around 280 nm and an emission peak at 500 and 530 nm at 298K and 77K, respectively. The wavelength shift is caused probably by vibronic peak

redistribution upon thermal broadening. The lifetimes for both complexes are also similar. The photoluminescence spectra of complex **3**, shows an excitation at 365 nm and an emission peak at 500 and 515 nm at 298 K and 77 K, respectively. The spectral profile for **3** shows a single emission in the green region assigned to ($T_1 \rightarrow S_0$) phosphorescence emission with lifetime of 11.24 and 19.26 μs at 298 K and 77 K, respectively, and ($S_0 \rightarrow T_1$) spin-forbidden excitation at λ_{max} = 365 nm. The microcrystalline sample of $[Ag(bpp)_2][BF_4]$, **3a**, at 298 K shows an excitation at 330 and 335 nm and an emission peak at 500 and 510 nm at 298 K and 77 K, respectively. Figure 9 shows photographs for colorless crystals of all complexes packed in Suprasil quartz tubes while being exposed to UV light by different wavelengths at room temperature and 77 K.

It is reasonable to assign the luminescence of all those complexes to ligand-centered luminescence sensitized by the heavy atom effect *via* the coordination to silver or copper atoms. However, unlike prior precedents whereby such $^3\pi$-π^* transitions occurred for monomers, as evident therein by observation of vibronic fine structure,[18,6g] we believe herein that the ligand-centered phosphorescence is due to aggregate emissions of π-stacked moieties, which is consistent with the crystal structures (*vide supra*). Further work, however, is warranted including elegant photophysical studies including time-resolved and steady-state measurements for solids vs temperature (down to 4 K *via* liquid He) and fluid and/or glassy solutions *vs* concentration for all complexes herein and the free ligand in order to more-accurately and quantitatively describe the photophysical processes, parameters, and validate or alter the aforementioned assignment.

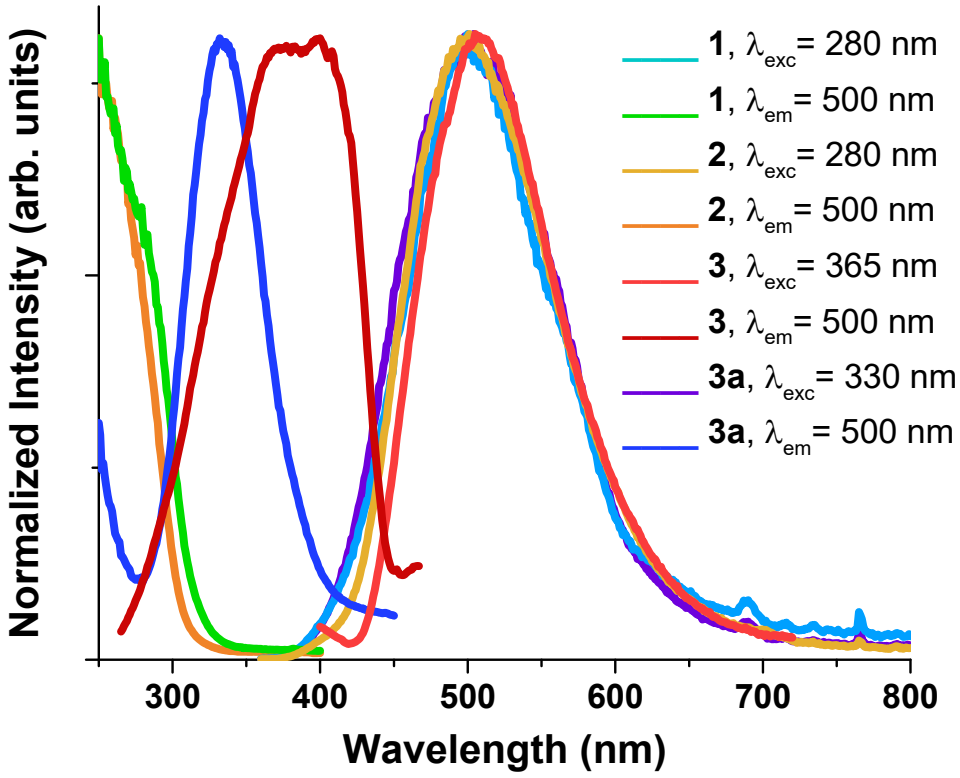

Figure 6. Solid-state emission and excitation spectra for all complexes at room temperature.

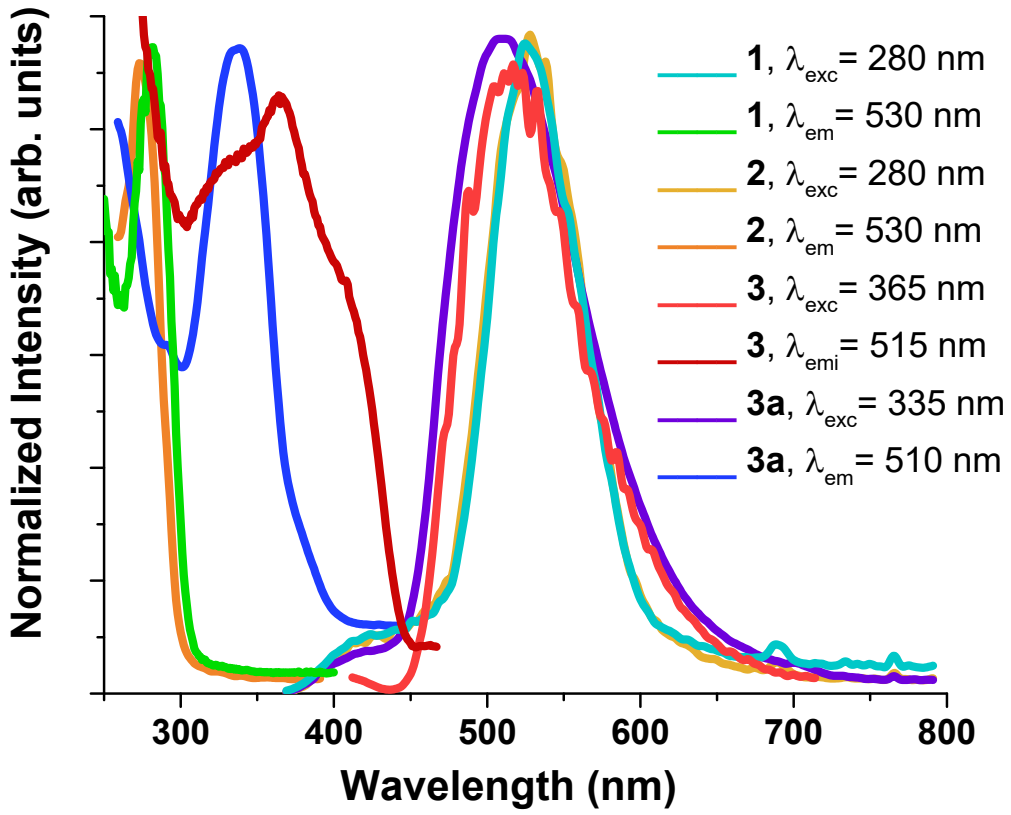

Figure 7. Solid-state emission and excitation spectra for all complexes at 77K.

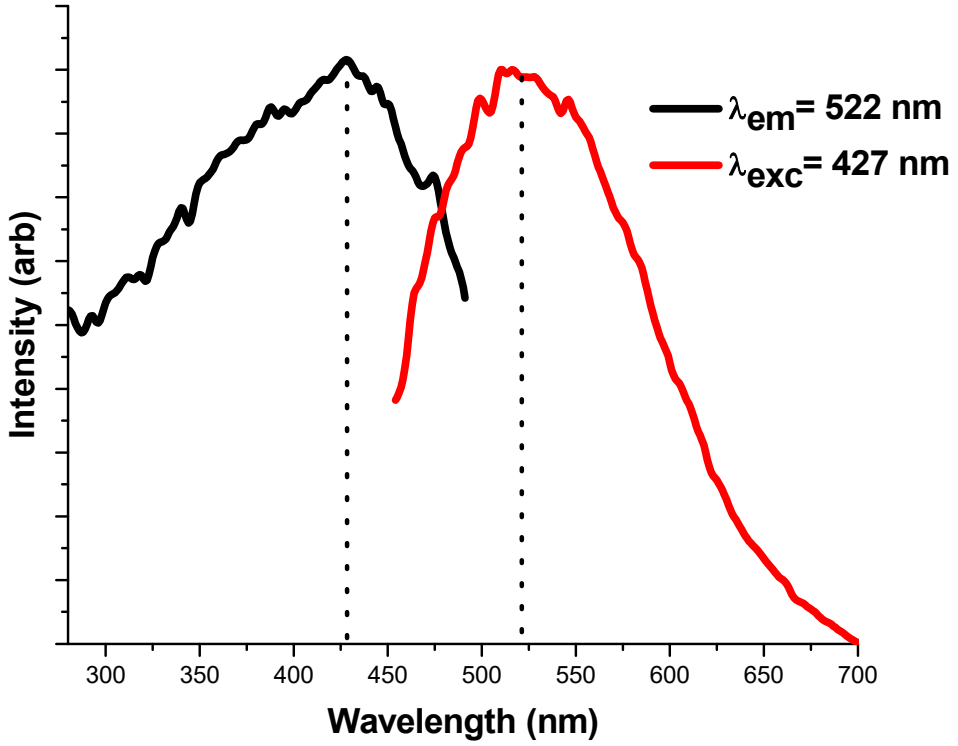

Figure 8. Solid-state emission and excitation spectra for bpp ligand only at 77 K.

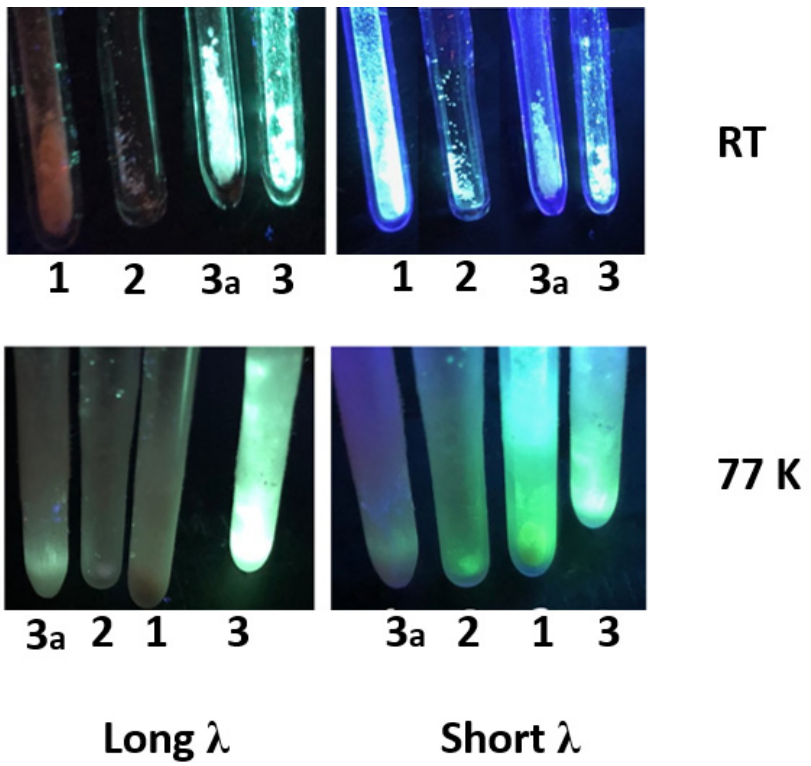

Figure 9. Photographs are shown as insets for colorless crystals packed in Suprasil quartz tubes while being exposed to UV light by different wavelengths at room temperature and 77 K for all complexes.

Commentary on Solventless vs Solvent-Mediated Reactions in this Class of Complexes.

The synthesis of complex herein represents a second case study from this family of complexes studied by the Rawashdeh-Omary group whereby a product has been obtained ONLY *via* solventless transformations, whereas solvent-mediated reactions failed to obtain the desired Cu(I) products but, instead, led to unidentifiable oxidized and/or reduced products; i.e., decomposed products likely consisting of Cu(II) complexes and/or Cu(0) metallic nanoparticles, respectively.

Shieh *et al.*, however, were able to synthesize the desired Cu(I) product, **3**, *via* a solvent-mediated-yet-unconventional synthetic route, using a mixed solvent (MeCN/EtOH) at 50 °C over 2 days, resulting in a yellow-green solution then, upon filtration and recrystallization at 4 °C, yellow-brown crystals with a mere 27% yield.[7] Our work by solventless reaction results in a white (with a light green tinge likely from room light-irradiated luminescence) product with a much higher 81% yield. Given the fact that the bpp ligand has broken conjugation between the two pyridyl rings, a white-colored solid/colorless solution major product is more likely. Thus, the low yield and colored products are likely due to Cu(II) impurities in the ref. 7 low-yield procedure. The scheme for this reaction using our approach is illustrated in Figure 10, whereby we deemed the solvent-mediated reaction unviable due to the fact that we did not pursue a low-yield route *via* our conventional single solvent-mediated synthesis. We note, however, that the opposite can also take place (i.e., reactions may proceed ONLY *via* solvent-mediated transformations, whereas solventless reactions have failed to obtain the desired products) or both the solvent-mediated and solventless routes have succeeded. Complex **3a** is an example for the previous statement. The difference between complex **3a** and complex **2** reported by Carlucci, *et al.*[3g] that their yield is between 30-50% but we found by our synthesis method that the yield can be more than 80% with a more conventional synthetic route that attains the product in 2 hrs instead of "some days" via the layering method in ref. 3g! For the work in this paper, the synthesis procedures of {[3,5-$(CF_3)_2Pz]_2(bpp)Ag_2\}_\infty$ (**1**) {[3,5-$(CF_3)_2Pz$][5-$(C_6F_5)Ttz$](bpp)Ag}$_\infty$ (**2**) and {$[Cu(bpp)_2][BF_4]\}_\infty$ (**3**) are straight-forward shown in Scheme 1 and the final products are air-stable, whereby products **1** and **2** have been obtained *via* solvent-mediated reactions while product **3** has been obtained by a solventless route (mechanical grinding). In the previous literature precedent (ref. 13), all three scenarios have been attained; we refer you to that reference for details. Finally, we caution,

however, that conventional crystal growth had to be invoked in both the solventless and solvent-mediated routes to obtain the crystal structures, hence somewhat ameliorating the scientific purity of the "green" claim for the solventless syntheses both herein and in ref. 13.

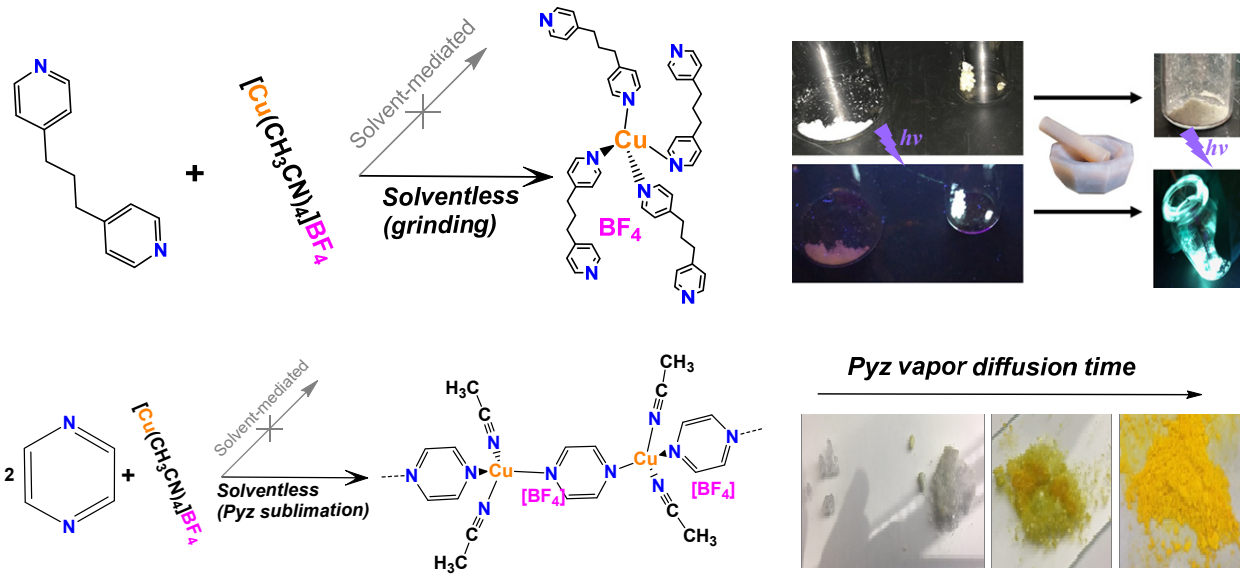

Figure 10. Illustration of two reaction schemes from this work (top) and ref. 13 (bottom) whereby a product has been obtained ONLY *via* a solventless transformation while solvent-mediated reactions failed to obtain the desired Cu(I) product.

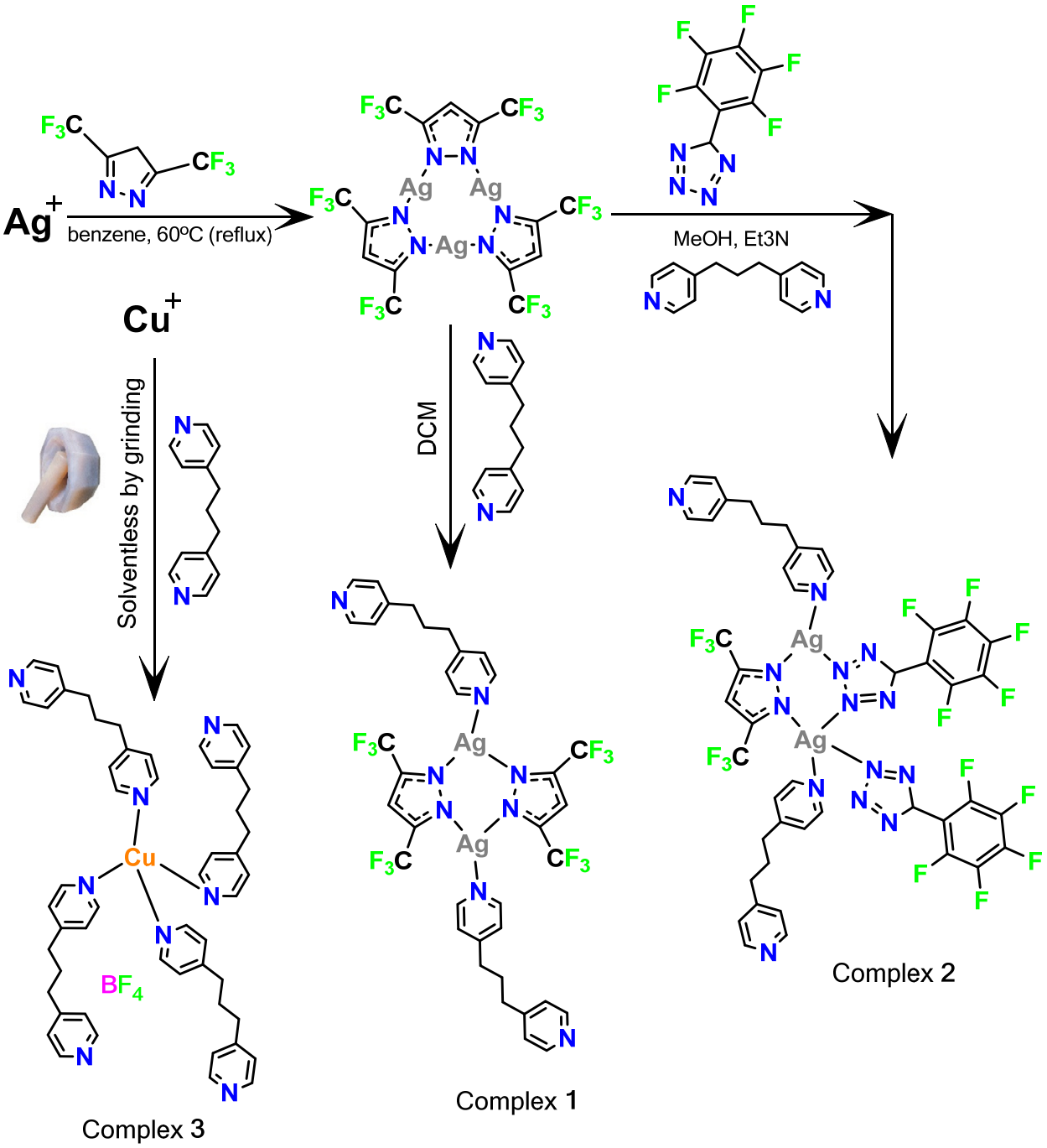

Scheme 1. Chemical transformations carried out in this work for complexes **1**-**3**.

Conclusions.

For complexes **1** and **2** which presents the azolate-based complexes, the starting material --the trinuclear Ag(I) complexe-- breaks down to dimer as expected upon coordinating the metal ions to the azolate and diimine ligands. Certain solvent molecules, such as acetonitrile was required to obtain single crystals with sufficient heating and sonication. The four different sites in the tetrazolate ligand lead to complicated geometry with a huge steric factor. Hence, only the tetrazolate/pyrazolate complex with bpp ligand which has the longest linker between the two pyridyl groups among the diimine ligands was successful. The reason is that the long linker in the bpp ligand gives the large silver atom more space and minimizes the steric effect to coordinate with other nitrogen atoms from the pyrazolate and tetrazolate ligands whereas the shorter linkers in the rest of the diimine ligands do not give the same advantage. In addition, back-to-back diimine ligands such as bpp play a significant role to form coordination polymers with extended chains. Mechanical grinding has been used under ambient laboratory conditions to carry out the reaction to attain the product, $\{[Cu(bpp)_2][BF_4]\}_\infty$, **(3)** that was monitored by gradual intensity changes as the reaction progresses by the exposure of UV light. Due to the instability of Cu(I) in solution, this product was unsuccessful to be synthesized in solvent-mediated reaction but, unexpectedly, by grinding the reactants, it forms a very stable product with a bright green luminescence.

Acknowledgements. This work was made possible by the Robert A. Welch Foundation (Grant B-1542 to M.A.O. and departmental grant to M.A.R.-O. at Texas Woman's University) and the National Science Foundation (CHE-1413641 to M.A.O.). We also acknowledge the NSF MRI Program (CHE-1726652) and the University of North Texas for supporting the acquisition of the Rigaku XtaLAB Synergy-S X-ray diffractometer.

Experimental Section

General Procedures. All manipulations were carried out under a purified nitrogen atmosphere using standard Schlenk techniques. The starting materials $\{[3,5\text{-}(CF_3)_2Pz]Ag\}_3$, and 5-(perfluorophenyl)-2H-tetrazole ($[5\text{-}(C_6F_5)Ttz]H$) were prepared by published methods from the literature.[4d,8,19] 1,3-bis(4-pyridyl)propane (bpp) was purchased and used as is from Sigma Aldrich. Dried and purified, ACS reagent grade solvents were used to carry out the synthesis. All glassware was oven-dried at 150 °C overnight. NMR spectra were recorded at 25 °C on an Oxford-400 Varian spectrometer (^1H, 400.4 MHz; ^{19}F, 470.62 MHz). Proton and fluorine chemical shifts are reported in parts per million (ppm) versus Me_4Si. NMR annotations used: br = broad, d = doublet, m = multiplet, s = singlet. Elemental analyses (C, H, and N) were performed in-house with a Fisons Instruments 1108 CHNS-O Elemental Analyzer for complexes **1** and **2**; and with a PerkinElmer 2400 Series II CHNS/O Elemental Analyzer System for complex **3**. Melting points were taken on an SMP3 Stuart Scientific Instrument. Infrared spectra were recorded on a Perkin-Elmer SPECTRUM ONE System FT-IR instrument from 4000 to 600 cm^{-1}. IR annotations used: br = broad, m = medium, mbr = medium broad, s = strong, sh = shoulder, w = weak.

*Synthesis of {[3,5-$(CF_3)_2$Pz]$_2$(bpp)Ag_2}$_\infty$ (**1**)*

To a stirring dichloromethane (10 mL) solution {[3,5-$(CF_3)_2$Pz]Ag}$_3$ (0.1 g, 0.10 mmol) and bpp (0.064 g, 0.30 mmol) (molar ratio 1:3). A white precipitate started to form instantly. The resulting solution was stirred for 2 hours and filtered. X-ray diffraction quality single crystals were grown during the slow evaporation of acetonitrile. The product isolated was not soluble in most organic solvents except acetonitrile. Yield~ 80%. ^{1}H NMR (Acetone-d^6, 298 K): δ 8.5 (s, 4H, C−H bpp), 7.3 (s, 1H, C−H pz), 7.3 (s, 4H, C−H bpp), 2. 9 (s, 2H, C−H_2 bpp), 1.99 (s, 1H, C−H_2 bpp). ^{19}F NMR (DMSO-d^6): δ −58.75 (s, C−F pz). M.p.: 405 ºC (dec). \ IR (cm^{-1}): 3012w (C-H bpp), 2855m (C-H bpp), 2328w (CN), 1939w, 1613s, 1502s, 1421s, 1339s, 1267s, 1010s. Anal. Calcd. for C_{23} H_{15} Ag_2 F_{12} N_6 : C, 33.73; H, 1.85; N, 10.26%. Found : C, 33.60 ; H, 1.89; N, 10.23 %.

*Synthesis of {[3,5-$(CF_3)_2$Pz][5-(C_6F_5)Ttz](bpp)Ag}$_\infty$ (**2**)*

To a stirring methanol (10 mL) and trimethylamine (1 mL) solution {[3,5-$(CF_3)_2$Pz]Ag}$_3$ (0.1 g, 0.10 mmol), [5-(C_6F_5)Ttz]H (0.026 g, 0.11 mmol) and bpp (0.064 g, 0.30 mmol) (molar ratio 1:1:3). A white precipitate started to form instantly. The resulting solution was stirred for 2 hours and filtered. X-ray diffraction quality single crystals were grown during the slow evaporation of acetonitrile. The product isolated was not soluble in most organic solvents but partially soluble in (DMF), (DMSO) and acetonitrile. The filtration of acetonitrile solution was required to get pure crystals. Yield: 79%. ^{1}H NMR (DMSO-d^6, 298 K): δ 9.1 (s, 4H, C−H bpp), 7.2 (s, 4H, C−H bpp), 6.95 (s, 1H, C−H pz), 2.6 (s, 2H, C−H_2 bpp), 1.9 (s, 1H, C−H_2 bpp). ^{19}F NMR (DMSO-d^6): δ −59.15 (s, C−F pz). M.p: 410 ºC (dec). IR (cm^{-1}): 3142w (C-H bpp), 2931m (C-H bpp), 2030w (CN), 1610s, 1505s, 1414s, 1364s, 1257s, 1118vs. Anal. Calcd. for C_{25} H_{15} Ag_2 F_{11} N_8: C, 35.24; H, 1.77; N, 13.15%. Found : C, 34.23 ; H, 1.72; N, 14.71 %.

Synthesis of {[Cu(bpp)$_2$][BF$_4$]}$_\infty$ ***(3)***

[Cu(CH$_3$CN)$_4$][BF$_4$] (0.1 g, 0.31 mmol) and 4,4′-trimethylenedipyridine (bpp) (0.15g, 0.75 mmol) were mixed and grinded in a vial. [Cu(MeCN)$_4$][BF$_4$] reacts with bpp by grinding resulting in a physical color change of the white copper precursor immediately to light green. Also, the luminescence properties change to bright green luminescence immediately shown via grinding; see Figure 10. The product was partially soluble in acetonitrile. The product was not soluble in most organic solvents. Using sonication and filtration is essential to acquire best result to recrystallization. X-ray diffraction quality single crystals were grown during the slow evaporation of acetonitrile. The filtration of acetonitrile solution was required to get pure crystals. Yield: 81%. ^{1}H NMR (Acetonitrile-*d*^{3}, 298 K): δ 8.54 (s, 4H, C−H bpp), 7.72 (s, 4H, C−H bpp), 2.51 (s, 2H, C−H$_2$ bpp), 2.24 (s, 1H, C−H$_2$ bpp). M.p.: 420-425 ºC (dec). IR (cm^{-1}): 3037m (C-H bpp), 2936m (C-H bpp), 2125w (CN), 1939w, 1601s, 1542m, 1527w, 1425m, 1415s, 1371w, 1217m, 1003s. Anal. Calcd. for C$_{26}$ H$_{28}$ Cu B F$_4$ N$_4$: C, 57.10; H, 5.16; N, 10.24%. Found (crystals): C, 57.22 ; H, 5.15; N, 10.16 %. Found (powder): C, 58.63 ; H, 5.19; N, 10.35 %.

Synthesis of {[Ag(bpp)$_2$][BF$_4$]}$_\infty$ ***(3a)***

To a stirring toluene (10 mL) solution of AgBF$_4$ (0.1 g, 0.51 mmol), bpp (0.20 g, 1.01 mmol) (molar ratio 1:2). A white precipitate starts to form instantly. The resulting solution was stirred for 2 hours and filtered. X-ray diffraction quality single crystals were grown during the slow evaporation of acetonitrile. The product isolated was not soluble in most organic solvents except acetonitrile. Yield > 80%. ^{1}H NMR (Acetone-*d*^{6}, 298 K): δ 8.47 (s, 4H, C−H bpp), 7.23 (s,

4H, C−H bpp), 2.69 (s, 2H, C−H_2 bpp), 2.34 (s, 1H, C−H_2 bpp). M.p.: 280 ºC. TGA of silver (% wt): 22.45% (calcd. 81.24%). IR (cm^{-1}): 3043m (C-H bpp), 2937m (C-H bpp), 2161w (CN), 1601s, 1582m, 1512w, 1443m, 1409s, 1365w, 1297w, 1211m, 1186m, 1051s. Anal. Calcd. for $C_{26}H_{28}AgBF_4N_4$: C, 52.82; H, 4.77; N, 9.48%. Found : C, 52.44 ; H, 4.36; N, 9.30 %.

Photophysical Measurements. Photoluminescence studies have been carried out for all four complexes isolated in this work, namely **1**, **2**, **3** and **3a**. The luminescence measurements were carried out for microcrystalline materials examined for purity for all three complexes. Steady-state luminescence spectra were acquired with a PTI QuantaMaster Model QM-4 scanning spectrofluorometer equipped with a 75-watt xenon lamp, emission and excitation monochromators, an excitation correction unit, a PMT detector, and an integrating sphere for direct quantum yield measurements. The excitation and emission spectra were corrected for the wavelength-dependent lamp intensity and detector response, respectively. Lifetime data were acquired using phosphorescence subsystem add-ons to the PTI instrument using a xenon flash lamp. Absorption spectra were acquired with a Perkin-Elmer Lambda 900 double-beam UV-vis-NIR spectrophotometer for solutions of crystalline samples prepared in ACS-grade acetonitrile using standard 1 cm quartz cuvettes.

X-Ray Crystallographic Determination. The X-ray data for compounds **1, 2** and **3a** were collected at 200(2) K and 220(2) K on a Bruker SMART APEX2 CCD-based X-ray diffractometer equipped with a low-temperature cryostat (Oxford Instruments) and a Mo X-ray tube (l = 0.71073 Å). Data collection, indexing, and initial cell refinements were carried out using APEX2,[20] with the frame integrations and final cell refinements carried out using SAINT.[21] An absorption correction was applied to each system using the program SADABS,[22] and all non-hydrogen atoms

were refined anisotropically. All hydrogen atoms were placed in idealized positions and were refined using a riding model. The structures were examined using the Addsym subroutine of PLATON in order to ensure that no additional symmetry could be applied to the finalized model.[23a] The structures were solved using SHELXS-97[23b] and refined using the SHELXL program package software.[24] The refinement details and structural parameters are summarized in Table 1.

Single crystal X-ray data for complex **3** was collected using a Rigaku XtaLAB Synergy-S diffractometer equipped with a HyPix-6000HE Hybrid Photon Counting (HPC) detector and dual Mo and Cu microfocus sealed X-ray source as well as a low-temperature Oxford Cryostream 800 liquid nitrogen cooling system at 100.0(1) K.

Data collection strategy was calculated within CrysAlisPro (1.171.40.12b; Rigaku Oxford Diffraction, 2018) to ensure desired data redundancy and percent completeness. Unit cell determination, initial indexing, data collection, frame integration, Lorentz-polarization corrections and final cell parameter calculations were carried out using CrysAlisPro. An absorption correction was performed using the SCALE3 ABSPACK scaling algorithm embedded within CrysAlisPro.

The single structure was solved using SHELXT,[25] all non-hydrogen atoms were refined anisotropically using SHELXL[24] and its space groups were unambiguously verified by PLATON.[26] All hydrogen atoms were attached via the riding model at calculated positions. Olex2 [27] was used for the preparation of the publication materials. Crystal data and refinement details are summarized in Table 1.

References:

1. (a) M. Du, C. P. Li, C. S. Liu, S. M. Fang, *Coord. Chem. Rev.,* **2013**, *257*, 1282. (b) F. Jin, Y. Zhang, H. Z. Wang, H. Z. Zhu, Y. Yan, J. Zhang, J. Y. Wu, Y. P. Tian, H.-P. Zhou, *Cryst. Growth Des.,* **2013**, *13*, 1978-1987. (c) V. Madhu, S. K. Das, *Cryst. Growth Des.,* **2014**, *14*, 2343. (d) Z. Zhang, M. J. Zaworotko, *Chem. Soc. Rev.,* **2014**, *43*, 5444. (e) P.-C. Cheng, C.-W. Yeh,; W. Hsu, T.-R. Chen, H.-W. Wang, J.-D. Chen, J.-C. Wang, *Cryst. Growth Des.,* **2012**, *12*, 943. (f) J. S. Hu, X. M. Zhang, H. L. Xing, J. He, J. J. Shi, *Mendeleev Commun.,* **2013**, *23*, 231 -232. (g) M. Hu, Z. W. Wang, H. Zhao, S. M. Fang, *Mendeleev Commun.,* **2015**, *25*, 150–152.

2. (a) L. R. MacGillivray, S. Subramanian, M. J. Zaworotko, *J. Chem. Soc., Chem. Commun.,* **1994**, 1325-1326. (b) M. J. Plater, M. R. St J. Foreman, A. M. Z. Slawin, Coordination Networks with 1,3-Bis(4-pyridyl)propane. *J. Chem. Research (S)*, **1999**, 2, 74-75. (c) D. Sun, D. F. Wang, N. Zhang, F. J. Liu, H. J. Hao, R. B. Huang, L. S. Zheng, *Dalton transactions*., **2003**, 2011-4-23. (d) J- J. Jiang, X- P. Li, X- L. Zhang, B- S. Kanga, C- Y. Su, *Cryst. Eng. Comm*., **2005**, *7*, 603-607.

3. (a) F. C. Pigge, *Cryst. Eng. Comm*., 2011, 13, 1733. (b) C. X. Ren, H. L. Zhu, G. Yang, X. M. Chen, *J. Chem. Soc., Dalton Trans.,* **2001**, 85. (c) M. L. Tong, X. M. Chen, B. H. Ye, L. N. Ji, *Angew. Chem., Int. Ed.,* **1999**, *38*, 2237. (d) L. Carlucci, G. Ciani, P. Macchi, D. M. Proserpio, S. Rizzato, *Chem.-Eur. J.,* **1999**, *5*, 237. (e) M. J. Plater, M. Foreman, T. Gelbrich, M. B. Hursthouse, *Cryst. Eng.,* **2001**, *4,* 319-328. (f) D. M. Ciurtin, Y. B. Dong, M. D. Smith, T. Barclay, H. C. Zur Loye, *Inorg. Chem.,* **2001**, *40*, 2825-2834. (g) L. Carlucci, G. Ciani, D. M. Proserpiob, S. Rizzato, *Cryst. Eng., Comm.* **2002**, *4*(22), 121–129.

4. (a) A. W. Freeman, S. C. Koene, P. R. L. Malenfant, M. E. Thompson, J. M. J. Frechet, *J. Am. Chem. Soc.,* **2000**, *122*, 12385–12386. (b) P. Furuta, J. Brooks, M. E. Thompson, J. M. J. Frechet, *J. Am. Chem. Soc.,* **2003**, *125*, 13165–13172. (c) P. Du, W. H. Zhu, Y. Q. Xie, F. Zhao, C.-F. Ku, Y. Cao, C. P. Chang, H. Tian, *Macromolecules,* **2004**, *37*, 4387–4398. (d) Z.-H. Zhao, H. Jin, Y.-X. Zhang, Z. Shen, D-.C. Zou, X.- H. Fan, *Macromolecules,* **2011**, *44*, 1405–1413.

5. P. S. Berdonosov, V. A. Dolgikh, *Russ. J. Inorg. Chem.,* **2008**, *53*, 1353–1358.

6. J. Wang, J.-G. Wang, X.-H. Li, H.-P. Xiao, *Transition. Met. Chem*., **2013**, *38*, 275–282.

7. M. Shieh, C.-C. Yu, C.-Y. Miu, C.-H. Kung, C.-Y. Huang, Y.-H. Liu, H.-L. Liu, C.-C. Shen, *Chem. Eur. J.*, **2017**, *23*, 11261–11271.

8. (a) C. V. Hettiarachchi, M. A. Rawashdeh-Omary, D. Korir, J. Kohistani, M. Yousufuddin, H. V. R. Dias, *Inorg. Chem.,* **2013**, *52*, 13576−13583. (b) M. A. Omary, C. Yang, (Denton TX., USA). Fluorinated Metal-Organic Frameworks for Gas Storage. US Patent 12/676555 November 11, 2010. (c) C. Yang, M. Messerschmidt, P. Coppens, M. A. Omary, *Inorg. Chem.,* **2006**, *45*, 6592−6594. (d) K. Fujisawa, Y. Ishikawa, Y. Miyashita, K.-I. Okamoto, *Chem. Letters.,* **2004**, *33,* 66-67. (e) M. A. Omary, M. A. Rawashdeh-Omary, M. W. A. Gonser, O. Elbjeirami, T. Grimes, T. R. Cundari, *Inorg. Chem.,* **2005**, *44*, 8200−8210. (f) H. V. R. Dias, H.V.K. Diyabalanage, M. G. Eldabaja, O. Elbjeirami, M. A. Rawashdeh-Omary, M. A. Omary, *J. Am. Chem. Soc.,* **2005**, *127*, 7489-7501. (g) M. A. Omary, M. A. Rawashdeh-Omary, H. V. K. Diyabalanage, H. V. R. Dias, *Inorg. Chem.,* **2003**, *42*, 8612−8614.

9. H. V. R. Dias, S. A. Polacha, Z. Wang, *J. Fluorine Chem.,* **2000**, *103*, 163-169.

10. M. A. Rawashdeh-Omary, M. D. Rashdan, S. Dharanipathi, O. Elbjeirami, P. Rameshb, H. V. R. Dias, *Chem. Commun.,* **2011**, *47*, 1160–1162.

11. (a) F. M. Libero, M. C. D. Xavier, F. N. Victoria, P. S. Nascente, L. Savegnago, G. Perin, D. Alves, *Tetrahedron. Letts.,* **2012**, *53*, 3091-3094. (b) G. F. Holland, J. N. Pereira, *J. Med. Chem.,* **1967**, *10*, 149–154. (c) K. Chauhan, P. Singh, V. Kumar, P. K. Shukla, M. I. Siddiqi, P. M. S. Chauhan, *Euro. J. Med. Chem.,* **2014**, *78*, 442-454. (d) P. B. Mohite, V. H. Bhaskar, *Int. J. PharmTech Res.,* **2011**, *3*, 1557-1566. (e) E. Łodyga-Chruscinska, *Coord. Chem. Rev.*, **2011**, *255*, 1824-1833. (f) E. A. Popova, R. E. Trifonov, V. A. Ostrovskii, *ARKIVOC,* **2012**, *2012*, 45-65. (g) G. Aromi, L. A. Barrios, O. Roubeau, P. Gamez, *Coord. Chem. Rev.*, **2011**, *255*, 485-546. (h) A. Bettencourt-Dias, P. S. Barber, S. Viswanathan, *Coord. Chem. Rev.,* **2014**, *165*, 273–274. (i) K. Darling, W. Ouellette, A. Prosvirin, S. Freund, K. R. Dunbar, J. Zubieta, *Cryst. Growth Des.,* **2012**, *12*, 2662–2672. (j) M.-G. Liu, P.-P. Zhang, J. Peng, H.-X. Meng, X. Wang, M. Zhu, D.-D. Wang, C.-L. Meng, K. Alimaje, *Cryst. Growth Des.,* **2012**, *12*, 1273–1281.

12. (a) R. N. Threlfall, A. G. Torres, A. Krivenko, M. J. Gait, M. H. Caruthers, *Org. Biomol. Chem.,* **2012**, *10*, 746. (b) E. Utagawa, A. Ohkubo, M. Sekine, K. Seio, *J. Org. Chem.,* **2007**, *72*, 8259-8266. (c) M. Greczmiel, P. Strohriegl, M. Meier, W. Brütting, *Macromolecules*, **1997**, *30*, 6042-6046. (d) H. Gerhards, A. Krest, P. J. Eulgem, D. Naumann, D. Rokitta, M. Valldor, A. Klein, *Polyhedron*, **2015**, *100*, 271–281.

13. (a) C. Adachi, M. A. Baldo, S. R. Forrest, *J. Appl. Phys.,* 2000, 87, 8049-8055. (b) V. V. Grushin, N. Herron, D. D. LeCloux, W. J. Marshall, V. A. Petrov, Y. Wang, *Chem. Commun.*, **2001**, *16*, 1494-1495. (c) J. Zhang, S. Kan, Y. Ma, J. Shen, W. Chan, C. Che, *Synth. Metals.,* **2001**,

121, 1723-1724. (d) H. V. R. Dias, H.-L. Lu, H.-J. Kim, S. A. Polach, T. K. H. H. Goh, R. G. Browning, C. J. Lovely, *Organometallics,* **2002**, *21*, 1466-1473. (e) H. V. R. Dias, H.-J. Kim, H.-L. Lu, K. Rajeshwar, N. R. de Tacconi, A. Derecskei-Kovacs, D. S. Marynick, *Organometallics,* 1996, 15, 2994-3003.

14. (a) R. Almotawa, G. Aljomaih, D. Trujillo, V.N. Nesterov, M. Rawashdeh-Omary, *Inorg. Chem.,* **2018**, *57*, 9962–9976. (b) O. Atoyebi, C. Brückner, *Inorg. Chem.,* **2019**, *58*, 15, 9631-9642. (c) H. M. Titi, J.-L. Do, A. J. Howarth, K. Nagapudi, T. Friščić, *Chem. Sci.,* **2020**, DOI: 10.1039/d0sc00333f.

15. H. Sigel, *Angew Chem.,* **1975**, *14*, 394.

16. (a) C.-C. Wang, S.-Y. Ke, C.-W. Cheng, Y.-W. Wang, H.-S. Chiu, Y.-C. Ko, N.-K. Sun, M.-L. Ho, C.-K. Chang, Y.-C. Chuang, G.-H. Lee, *Polymers,* **2017**, *9*, 644. (b) Y. B. Dong, M. D. Smith, R. C. Layland, H. C. zur Loye, *Chem. Mater.,* **2000**, *12*, 1156–1161. (c) Y. B. Dong, M. D. Smith, H. C. zur Loye, *Inorg. Chem.,* **2000**, *39*, 4927–4935. (d) Y. B. Dong, M. D. Smith, H. C. zur Loye, *J. Solid State Chem.,* **2000**, *155*, 143–153. (e) S. Parshamoni, S. Konar, *Cryst. Eng. Comm.,* **2016,** *18*, 4395–4404. (f) S. Parshamoni, S. Sanda, H. S. Jena, S. Konar, *Chem. Asian. J.,* **2015**, *10,* 653–660. (g) E. Tahmasebi, M. Y. Masoomi, Y. Yamini, A. Morsali, *Inorg. Chem.,* **2015**, *54*, 425–433. (h) B. Bhattacharya, D. K. Maity, R. Mondal, E. Colacio, D. Ghoshal, *Cryst. Growth Des.,* **2015**, *15*, 4427–4437. (i) B. Manna, S. Singh, A. Karmakar, A. V. Desai, S. K. Ghosh, *Inorg. Chem.,* **2015**, *54*, 110–116. (j) B. Bhattacharya, R. Haldar, D. K. Maity, T. K. Maji, D. Ghoshal, *Cryst. Eng. Comm.,* **2015**, *17*, 3478–3486. (k) V. Safarifard, S. Beheshti, A. Morsali, *Cryst. Eng. Comm.,* **2015**, *17*, 1680–1685. (l) D. K. Maity, B. Bhattacharya, R. Mondal, D. Ghoshal, *Cryst. Eng. Comm.,* **2014**, *16*, 8896–8909. (m) B. Bhattacharya, R. Haldar, R. Dey, T. K.

Maji, D. Ghoshal, *Dalton. Trans.,* **2014**, *43*, 2272–2282. (n) R. Dey, B. Bhattacharya, P. Pachfule, R. Banerjee, D. Ghoshal, *Cryst. Eng. Comm.,* **2014**, *16*, 2305–2316. (o) M. Y. Masoomi, K. C. Stylianou, A. Morsali, P. Retailleau, D. Maspoch, *Cryst. Growth Des.,* **2014**, *14*, 2092–2096. (p) S. Parshamoni, S. Sanda, H.S. Jena, K. Tomar, S. Konar, *Cryst. Growth Des.,* **2014**, *14*, 2022–2033. (q) J. Zhou, L. Du, Y. F. Qiao, Y. Hu, B. Li, L. Li, X.Y. Wang, J. Yang, M .J. Xie, Q. H. Zhao, *Cryst. Growth Des.,* **2014**, *14,* 1175–1183. (r) B. Bhattacharya, D. K. Maity, P. Pachfule, E. Colacio, D. Ghoshal, *Inorg. Chem. Front.,* **2014**, *1*, 414–425. (s) B. Bhattacharya, R. Dey, D. K. Maity, D. Ghoshal, *Cryst. Eng. Comm*., **2013**, *15*, 9457–9464. (t) *Polymers.* **2017**, *9*, 644. (u) S. Sanda, S. Parshamoni, A. Adhikary, S. Konar, *Cryst. Growth Des.,* **2013**, *13*, 5442–5449. (v) B. Bhattacharya, R. Dey, P. Pachfule, R. Banerjee, D. Ghoshal, *Cryst. Growth Des.,* **2013**, *13*, 731–739. (w) S.-Q. Zhang, F.-L. Jiang, M.-Y. Wu, J. Ma, Y. Bu, M.-C. Hong, *Cryst. Growth Des.,* **2012**, *12*, 1452–1463.

17. (a) J.-C. Jin, Y.-Y. Wang, W.-H. Zhang, A. S. Lermontov, E. K. Lermontova, Q.-Z. Shi, *Dalton Trans.,* **2009**, 46, 10181-10191. (b) P. Horcajada, R. Gref, T. Baati, P. K. Allan, G. Maurin, G. Couvreur, P. Férey, R. E. Morris, C. Serre, *Chem. Rev.,* **2011**, *112*, 1232-1268.

18. (a) M. A. Omary, O. Elbjeirami, C. S. P. Gamage, K. M. Sherman, H. V. R. Dias, *Inorg. Chem.,* **2009**, *48*, 5, 1784-1786. (b) M. A. Omary, O. Elbjeirami, M. A. Rawashdeh-Omary*, Res. Chem. Intermed.*, **2011**, *37*, 691-703. (c) M. A. Rawashdeh-Omary, *Comments Inorg. Chem.,* **2012**, *33*, 88-101. (d) O. Elbjeirami, M. D. Rashdan, V. Nesterov, M. A. Rawashdeh-Omary, *Dalton Trans*., **2010**, *39*, 9465-9468.

19. G. J. Kubas, *Inorg. Synth*., **1979**, *19*, 90.

20. Bruker APEX2; Bruker Advanced Analytical X-ray Systems, Inc. Copyright 2007, Madison, WI.

21. Bruker Saint; Bruker Advanced Analytical X-ray Systems, Inc. Copyright 2007, Madison, WI.

22. Bruker SADABS; Bruker Advanced Analytical X-ray Systems, Inc. Copyright 2007, Madison, WI.

23. (a) A.L. Spek, PLATON: A Multipurpose Crystallographic Tool, Utrecht University, 456 Utrecht, The Netherlands, 2006. (b) Sheldrick, G. M. SHELXTL, v. 2008/3; Bruker Analytical X-ray: Madison, WI, 2008.

24. G. M. Sheldrick, "Crystal structure refinement with SHELXL", *Acta Cryst.,* **2015**, *C71*, 3-8

25. G. M. Sheldrick, "SHELXT--Integrated space-group andCrystal structure determination", *Acta Cryst.,* **2015***, A71*, 3-8.

26. A. L. Spek, "Structure validation in chemical crystallography", *Acta Cryst.,* **2009**, *D65*, 148-155.

27. O. V. Dolomanov, L. J. Bourhis, R. J. Gildea, J. A. K. Howard, H. Puschmann, *J. Appl. Cryst.,* **2009**, *42*, 339-341.